Computational and Theoretical Chemistry 1025 (2013) 1–7

Contents lists available at ScienceDirect

Computational and Theoretical Chemistry

journal homepage: www.elsevier.com/locate/comptc

Computational studies on the catalytic mechanism of phosphoketolase

Jing Zhang [a,b], Yongjun Liu [a,c,*]

[a] Northwest Institute of Plateau Biology, Chinese Academy of Sciences, Xining, Qinghai 810001, China
[b] Key Laboratory of Inorganic Chemistry in Universities of Shandong (Jining University), Qufu, Shandong 273155, China
[c] School of Chemistry and Chemical Engineering, Shandong University, Jinan, Shandong 250100, China

ARTICLE INFO

Article history:
Received 1 August 2013
Received in revised form 27 September 2013
Accepted 27 September 2013
Available online 5 October 2013

Keywords:
Phosphoketolase
Density functional theory (DFT) method
Reaction mechanism
THDP-dependent enzyme
Dehydration
Keto–Enol tautomerism

ABSTRACT

Phosphoketolase (PK) is a thiamine diphosphate (THDP) dependent enzyme which plays key roles in the metabolism of heterofermentative bacteria. By using density functional theory (DFT) method, the catalytic mechanism of PK has been studied on simplified models. The calculation results indicate that the formation of 2-α,β-dihydroxyethylidene-THDP (DHETHDP) and erythrose-4-phosphate (E4P) involves one C–C bond formation and one C–C bond cleavage process. Each C–C bond formation or cleavage is always accompanied by a proton transfer in a concerted but asynchronous way. The dehydration process in the reaction of PK is distinct from that of other THDP-dependent enzymes. The Keto–Enol tautomerism process is assisted with a mediator His553. His64, His553 and His97 are found to have the function to stabilize the transition states and intermediates. His64 is a better candidate of B1 catalyst. His553 acts as a proton donor to protonate the carbonyl oxygen, and plays intermediary role in the Keto–Enol tautomerism process. His97 is the probable B2 catalyst in the dehydration process.

1. Introduction

Phosphoketolase (PK) is a prominent enzyme in sugar metabolism, which requires thiamine diphosphate (THDP) and a bivalent cation as cofactors for enzymatic activity [1–4]. PK mainly plays roles in the metabolism of heterofermentative bacteria, and functions as key enzyme in two pathways. One pathway is the phosphoketolase pathway (PK pathway), which is the central pathway in the metabolism of heterofermentative lactic acid bacteria including the genera Lactobacillus and Leuconostoc [5]. The other is the fructose-6-phosphate (F6P) shunt pathway called "bifid shunt" [6]. PK can catalyze the formation of acetyl phosphate (AcP) and erythrose-4-phosphate (E4P) from fructose-6-phosphate (F6P), or the formation of AcP and glyceraldehyde 3-phosphate (G3P) from xylulose-5-phosphate (X5P) utilizing inorganic phosphate (Pi) as acceptor, as shown in the following overall reactions (1) and (2) [7]:

$$\text{fructose-6-phosphate (F6P)} + \text{Pi} \rightarrow \text{erythrose-4-phosphate (E4P)} + \text{acetyl-phosphate (AcP)} \quad (1)$$

$$\text{xylulose-5-phosphate (X5P)} + \text{Pi} \rightarrow \text{glyceraldehyde-3-phosphate (G3P)} + \text{acetyl-phosphate (AcP)} \quad (2)$$

According to substrate preference, PK is divided into two types, namely XPK (EC 4.1.2.9) when specificity is for X5P, and XFPK (EC 4.1.2.22) when both X5P and F6P are accepted [8]. XPK is a key enzyme in the PK pathway of various microbes, but XFPK is only found in bifidobacteria and can catalyze the two steps in the "bifid shunt" pathway owing to its dual-substrate specificity [4]. Another THDP dependent enzyme catalyzing the key step of "bifid shunt" pathway is transketolase (TK), which together with PK belongs to TK family when THDP dependent enzymes are divided into four families based on their primary and tertiary structures [9]. In the past decades, many experimental and theoretical researches have been made for understanding the properties of TK [10–13]. But PK has been little studied since its distribution in the natural world is not very widespread compared with TK [3].

In 2010, the high resolution crystal structures of XFPK from bifidobacterium longum (PDB code: 3AI7) and bifidobacterium breve (PDB code: 3AHC, etc.) were determined [3,4]. These three-dimensional structures provide new insights into the fold of phosphoketolases, binding mode of cofactors, and information of catalytic reaction. PK is a dimeric molecule, which is the functional unit of the enzyme (shown in Fig. 1) [14,15]. Each subunit consists of three domains, including the N-terminal domain (residues 2–378), the middle domain (residues 379–612) and the C-terminal domain (residues 613–814). Residues from both subunits build up two related active sites that are involved in the binding of cofactor THDP. From the active center of Bifidobacterium Longum PK shown in Fig. 2a, we can see that this enzyme shares some similarities with most other THDP enzymes [16–21]. Firstly, THDP adopts the V-like

* Corresponding author at: School of Chemistry and Chemical Engineering, Shandong University, Jinan, Shandong 250100, China. Tel.: +86 531 883 655 76; fax: +86 531 885 644 64.
E-mail address: yongjunliu_1@sdu.edu.cn (Y. Liu).

2210-271X/$ - see front matter © 2013 Elsevier B.V. All rights reserved.
http://dx.doi.org/10.1016/j.comptc.2013.09.026

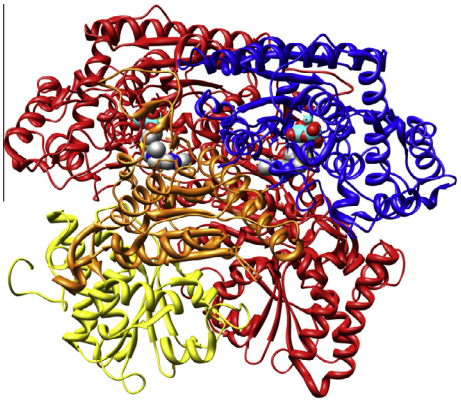

Fig. 1. The overall structure of PK. One subunit is color-coded red. For the other subunit, the three domains are color-coded differently: N-terminal domain is blue, middle domain is orange and C-terminal domain is yellow. Two THDP cofactors are shown as spheres. (For interpretation of the references to color in this figure legend, the reader is referred to the web version of this article.)

conformation to bring the N4′-amino group of the pyrimidine ring adjacent to the C2 of the thiazolium ring, greatly facilitating the formation of ylide to initiate the catalytic cycle. Secondly, a universally conserved glutamate residue (Glu479) forms a hydrogen bond with the N1′ atom of THDP. It is important to note that PK and TK have similar active site structures in spite that the sequence identity between them is only 17.1%. Several histidine residues in the active site as well as other residues important for catalysis are completely conserved between PK and TK [4].

A possible mechanism of PK has been proposed by Yevenes and Frey [7,22], as shown in Scheme 1. Similar with other THDP-dependent enzymes, THDP must be activated firstly to form THDP ylide to initiate the catalytic cycle. A proton is transferred from the side-chain of carboxyl group of Glu479 to N1′-nitrogen of aminopyridine ring, which aids amino-imino tautomerization at 4′-NH2, and the imino group extracts a proton from the C2-carbon of the thiazolium group (step0). Then, the catalytic cycle starts with the nucleophilic attack of the deprotonated C2-carbon of THDP ylide at the C2″ carbonyl carbon atom of the substrate sugar (F6P or X5P), producing the first covalent intermediate THDP-F6P or THDP-X5P (step1). Next, the scissile C2″–C3″ bond of the sugar moiety of THDP-F6P or THDP-X5P is broke to generate 2-α,β-dihydroxyethylidene-THDP (DHETHDP), and the first product (E4P or G3P) is liberated from the enzyme (step2). A proton acceptor B1 is required to deprotonate the C3″ hydroxyl group of the THDP-F6P or THDP-X5P in this step. The third step is the dehydration process of DHETHDP which requires a proton donor (B2) to protonate the C1″ hydroxyl group (step3). A water molecule is released and enolacetyl-THDP is formed. Enolacetyl-THDP is then converted to 2-acetyl-thiamine pyrophosphate (AcTHDP) by a transformation of enol and ketone (step4). Finally, inorganic phosphate (Pi) attacks the AcTHDP to form acetyl-phosphate (AcP) and the THDP ylide is regenerated (step5). The reaction of PK is distinct from that of other THDP-dependent enzymes at the dehydration process. In the case of TK, the elimination of water from DHETHDP does not occur. Instead, DHETHDP intermediate combines with the incoming aldose to yield a ketose with an extended carbon skeleton.

Some experimental advances have been achieved in understanding the catalytic mechanism of PK. Takahashi et al. [3] superimposed the structures of PK with THDP and TK in complex with THDP-F6P (PDB code: 2R8P) to generate the docking model of PK with THDP-F6P. The docking model suggests that His64 or His320 are possible B1 catalyst that extracts a proton from C3″-hydroxyl group of the sugar moiety of THDP-F6P, while His142 or His553 could be the B2 catalyst that causes the elimination of water from DHETHDP. Shortly afterwards, Suzuki et al. [4] reported the crystal structures of the two intermediates before and after dehydration (DHETHDP and AcTHDP). Observation of the DHETHDP and AcTHDP supports the previous notion that the dehydration occurs in the absence of Pi [7]. Mutagenesis and crystallographic analysis of PK indicate that the most possible candidate of B1 catalyst is His64. But the B2 catalyst remains unclear, and the possible residues are assigned to be His553, the N4′ group of the pyrimidine, or His97. These studies expanded the structural insight into the reaction mechanism of PK, but many questions still remain to be settled besides the assignment of B1 and B2 catalysts. The detailed description of each elementary step, the roles of key pocket residues involved in proton transfer and stabilization of reaction intermediates and transition states, and the energetics of the whole reaction are still not fully understood.

In the present work, we perform a theoretical study on the catalytic mechanism of PK (steps1–4) using hybrid density functional theory (DFT) method on simplified models, which has been successfully employed to study enzymatic systems and gain lots of mechanistic insights [23,24]. Based on the crystal structure of the wild type Bifidobacterium Longum XFPK (PDB code: 3AI7) determined by Takahashi et al. [3] with F6P as substrate, the computational models were constructed, and the residues acting as B1 or B2 catalyst were assigned. In addition, the reaction barriers and energies were calculated.

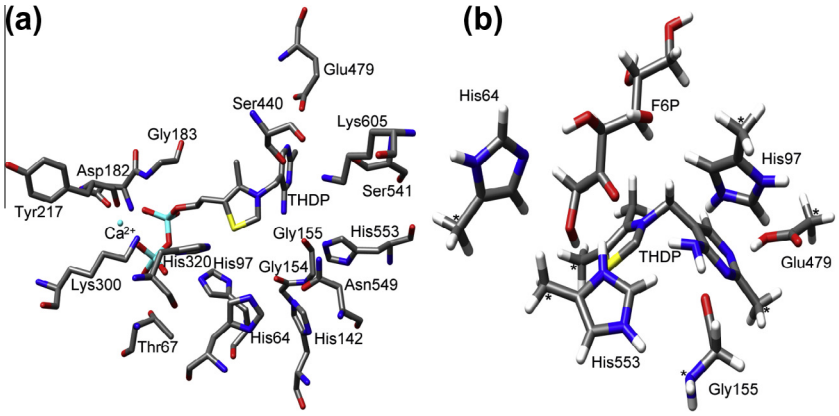

Fig. 2. (a) The active site of PK with the cofactors THDP and Ca^{2+} (PDB code 3AI7). (b) The calculation model employed in the present work. The F6P molecule is separately optimized and then deposited into the active pocket using the Autodock program. The fixed atoms are labeled by asterisks.

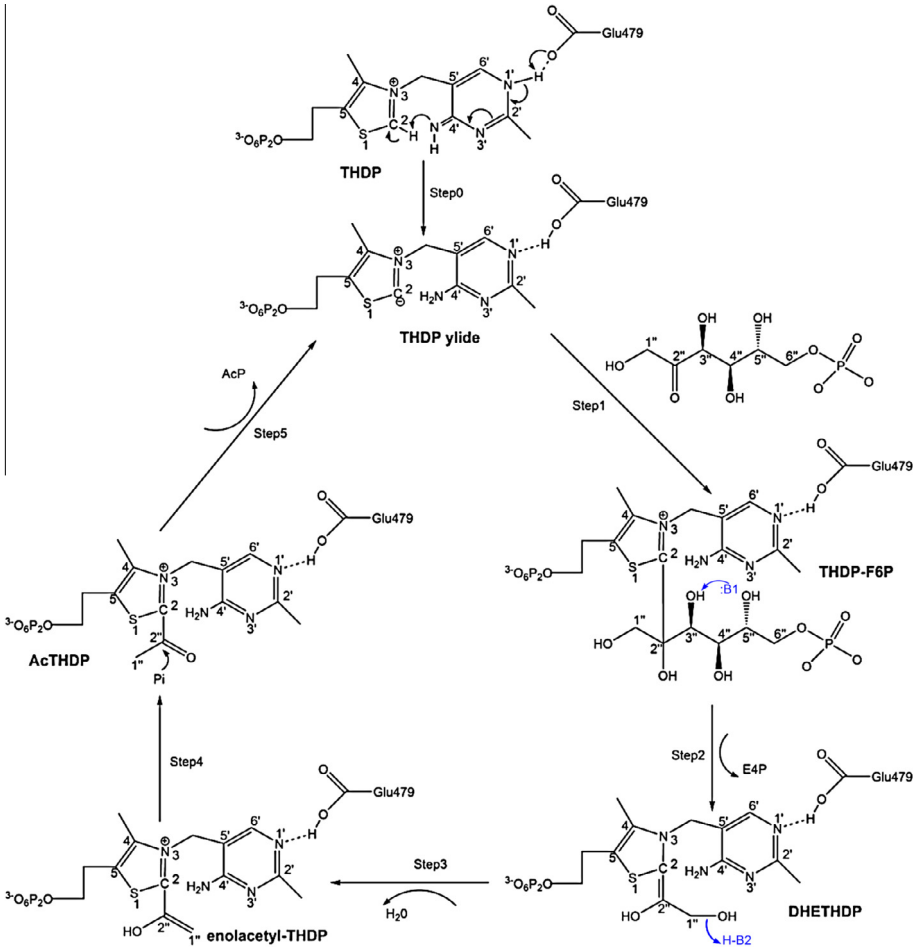

Scheme 1. Proposed catalytic mechanism of PK for the formation of AcP and E4P utilizing F6P and Pi as substrates.

2. Computational details

All calculations were performed by using the B3LYP density functional theory method as implemented in Gaussian03 software package [25]. Geometry optimizations were carried out at the level of 6-31G(d,p) basis set. The F6P molecule was separately optimized and then placed into the active site using the Autodock program [26]. Some truncated atoms were fixed to their crystallographic positions to prevent unrealistic movements of the groups during the optimization. More accurate energies were obtained by single-point calculations using the larger 6-311++G(2d,2p) basis set on the optimized geometries. Frequencies were calculated at the same level of theory as the geometry optimizations to confirm the nature of the stationary points and also to obtain zero-point energies (ZPE). Fixing coordinates introduces a few small negative eigenvalues, in this case all below 30i cm^{-1}. These frequencies do not contribute significantly to the ZPE and can be ignored. To consider the polarization effects of enzyme environment on the energetics of each reaction step, we also used the polarizable-continuum model (PCM) [27,28] with a dielectric constant of 4 to calculate the single point energies at 6-311++G(2d,2p) level for each species on the optimized geometries [29–33]. All the transition states were confirmed by intrinsic reaction coordinate (IRC) calculations.

3. Results and discussions

Now that the activation mechanism of THDP has been extensively studied elsewhere [34–37], THDP ylide was chosen as the beginning form in our computational model. Experimental studies have proved that the universally conserved residue Glu479 plays a key role in activating THDP and is essential for the PK activity [7,38]. The carbonyl oxygen atom of Gly155 forms hydrogen bond to 4′-NH_2 of THDP. In addition, experimental studies show that the most possible candidate of B1 catalyst is His64, and the possible B2 catalyst are assigned to be His553, the N4′ group of the pyrimidine, or His97. His142 and His320 are excluded from the candidates of B1 and B2 catalysts on the basis of mutagenesis and crystallographic analysis. Therefore, Glu479, Gly155, His 64, His 553 and His 97 were included in the calculation model (shown in Fig. 2b). As shown in Fig. 2b, the side chains of these residues were truncated to decrease the computational consumption, and the truncated atoms (asterisks in Fig. 2b) were fixed to their crystallographic positions during the optimizations. The terminal and truncated carbon atoms of THDP ylide were frozen to keep the V-like conformation of the THDP. This strategy is different from that of the earlier studies [39,40], but it also can keep the V-conformation of the THDP and maintain the middle moiety of THDP flexible. The torsion angles Φ_T from the four atoms C5′–C3,5′–N3–C2 and Φ_P from the atoms C4′–C5′–C3,5′–N3 for defining the orientation of THDP rings in all species will be given in the corresponding figures.

3.1. DHETHDP formation and E4P dissociation

As shown in Scheme 1, the formation of DHETHDP intermediate and E4P requires two steps (step1 and step2). In our calculations, IM1 and IM2 are the simplified models of THDP-F6P and DHETHDP, respectively. The optimized structures of initial reactant (R),

transition states (TS1 and TS2) and intermediates (IM1 and IM2) are shown in Fig. 3.

From Fig. 3 we can see that in reactant (R) the substrate F6P is stabilized by two hydrogen bonds from His97 and His64. The hydrogen bond length (r8) between His64 and the C3″ hydroxyl group of F6P is relatively long (2.05 Å) while that of His97 with the carbonyl group of F6P is very short (1.83 Å, not shown in Fig. 3). The C2 carbanion of thiazole ring is far from the C2″ of F6P (r1, 3.94 Å). In transition state (TS1), the C2–C2″ distance changes to 2.36 Å (r1) from 3.94 Å, and the distance (r3) of hydrogen atom of His553 with the carbonyl oxygen atom changes to 1.71 Å from 4.29 Å. But the proton transfer from the His553 to the carbonyl oxygen does not start yet, i.e., the proton to be transferred is still at His553. In IM1, the C2–C2″ bond is formed with a distance of 1.55 Å (r1), and the proton transfer from His553 to carbonyl oxygen is completed. From the structures of R, TS1 and IM1, we can see that the ligation of C2–C2″ bond and the proton transfer from His553 to the carbonyl group of F6P is a concerted process but not precisely synchronous. The start of proton transfer is much later than the ligation of C2–C2″ bond. In addition, the hydrogen bond length (r8) between His64 and the C3″ hydroxyl group of F6P is 2.17 Å in IM1, which will favor the next proton transfer.

As shown in Scheme 1 and Fig. 3, the next step is the cleavage of C2″–C3″ carbon bond (r5) of THDP-F6P together with the proton transfer from the C3″ hydroxyl group of THDP-F6P to the proton acceptor (His64) to generate DHETHDP carbanion/enamine intermediate (IM2) and release the first product E4P via TS2. In TS2, the C2″–C3″ distance (r5) changes from 1.61 Å to 2.12 Å, meanwhile, the proton of the C3″ hydroxyl group transfers to His64, which is marked by the change of r8 from 2.17 Å to 1.09 Å. In IM2, the C2″–C3″ carbon bond (r5) further elongated from 2.12 Å to 3.50 Å, which means the C2″–C3″ bond has completely broken. By comparing the structures of IM1, TS2 and IM2, one can see that this elementary reaction occurs in a concerted asynchronous mechanism, i.e., the proton transfer is almost finished in TS2 while the C2″–C3″ bond is on the way to be broken. Moreover, C2–C2″ carbon bond (r1) changes from single to double bond during this step, which agrees well with the proposed mechanism. It is worth noting that our calculations further confirm the experimental speculation that His64 is a better candidate of B1 catalyst. In addition, they also interpret the reason why an adduct-free THDP is trapped by the H553A mutation is that His553 acts as a proton donor to protonate the carbonyl oxygen in step1 [4].

The energy profile is shown in Fig. 4. To consider the polarization effects of enzyme environment on the energy barriers, the polarizable-continuum model (PCM) single point calculations at the level of 6-311++G(2d,2p) basis set were further performed on the optimized structures. The calculated energy barriers on the PCM model for the formation of IM1 and IM2 are 11.97 and 14.98 kcal/mol, implying that both of the two steps are easy to occur. The energy barriers in gas phase are 7.66 and 16.95 kcal/mol, indicating the enzyme environment imposes significant but different influences on each elementary step. The same effect was also found in other steps.

3.2. Dehydration

The next step (step3 in Scheme 1) is the dehydration process of DHETHDP which is different from other well studied THDP-dependent enzymes [13,18,20,41]. The C1″ hydroxyl group is protonated by a proton donor B2 to form a water molecule and generate enolacetyl-THDP.

After the first product E4P was removed from IM2, IM3 was obtained, as shown in Fig. 5. From IM3 we can see that, the possible B2 catalyst is His97, and the distance between the hydrogen of His97 and the O atom of C1″ hydroxyl group (r3) is 1.61 Å, which is favorable for proton transfer. In transition state TS3, r3 changes to 1.12 Å from 1.6 Å. The C–O bond (r2) changes to 1.73 Å from 1.48 Å. In IM4, the C–O bond has completely broken and the water molecule is released. The energy profile is shown in Fig. 4. We noted that the energy barrier for the formation of enolacetyl-THDP (IM4) is lower than that of the formation of DHETHDP (IM2 and

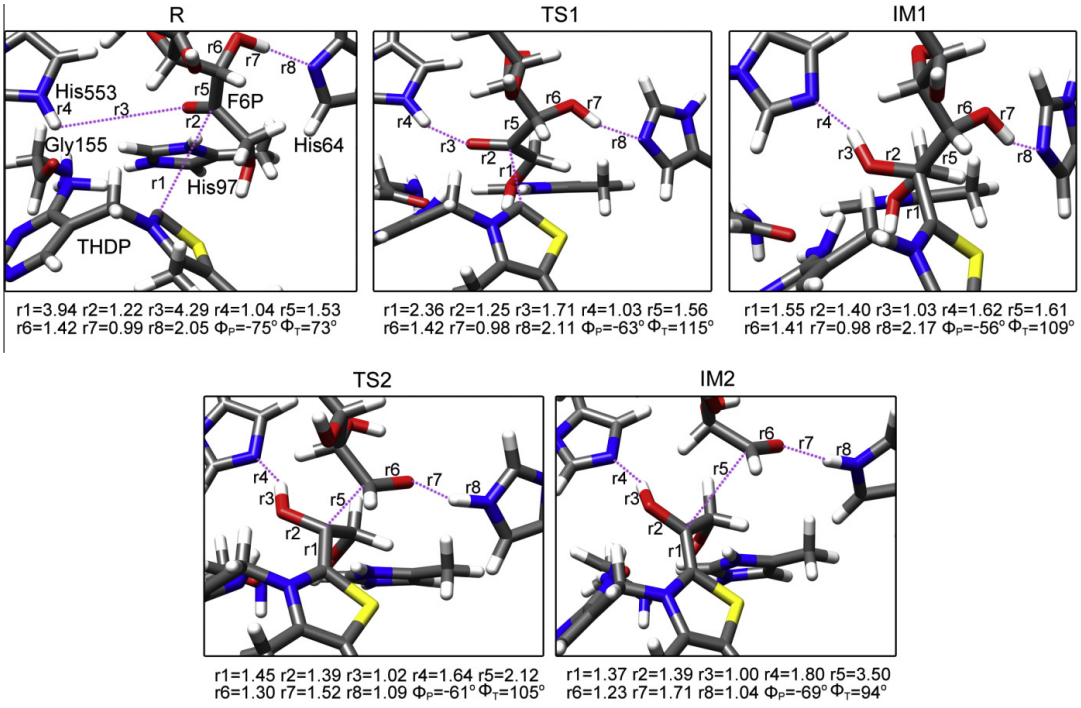

Fig. 3. The truncated active center of the optimized geometries for various species in the process of DHETHDP formation and E4P dissociation obtained at the B3LYP/6-31G(d,p) level. The key bond distances are shown in angstrom and characteristic torsion angles Φ_T and Φ_P for the orientation of the THDP rings are shown in degree.

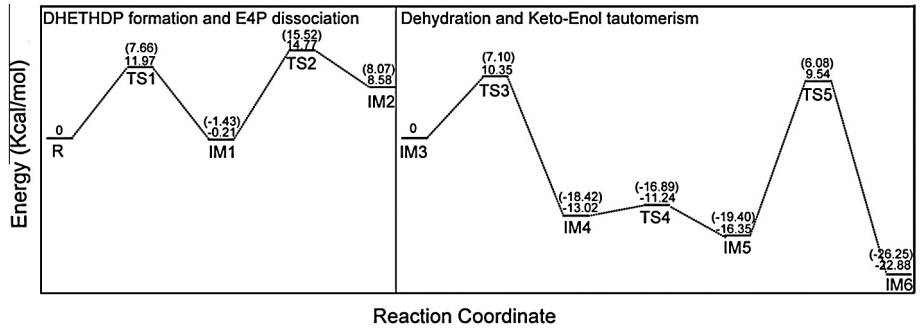

Fig. 4. Energy profile for the pK catalytic process (steps1–4). The ZPE-corrected relative energies obtained at the B3LYP/6-311++G(2d,2p)//B3LYP/6-31G(d,p) level in solution phase and gas phase (values in parentheses) are given in kcal/mol.

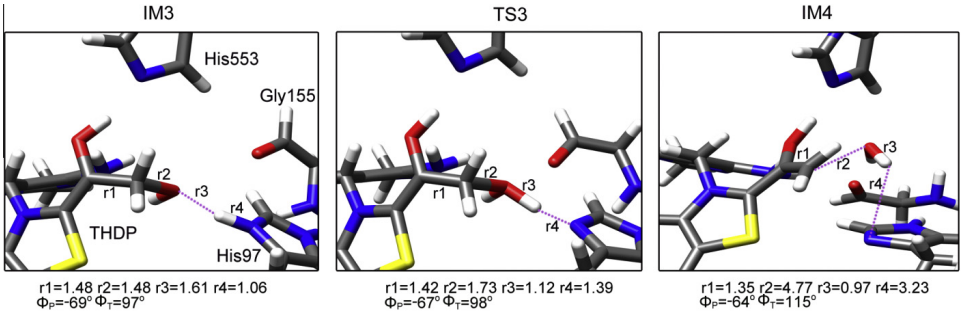

Fig. 5. The truncated active center of the optimized geometries for various species in the dehydration process of DHETHDP obtained at the B3LYP/6-31G(d,p) level. The key bond distances are shown in angstrom and characteristic torsion angles Φ_T and Φ_P for the orientation of the THDP rings are shown in degree.

IM3) (10.35 *vs.* 15.98 kcal/mol). The relative energy of IM4 is 13.02 kcal/mol lower than that of IM3, meaning the intermediate enolacetyl-THDP (IM4) is relatively stable and DHETHDP (IM2 and IM3) is easy to dehydrate and form enolacetyl-THDP. All of these calculation results agree well with the experimental observation of Suzuki et al. [4]. Our calculations also verify that His97 is the favorable B2 catalyst, which cannot be easily identified by experiment alone.

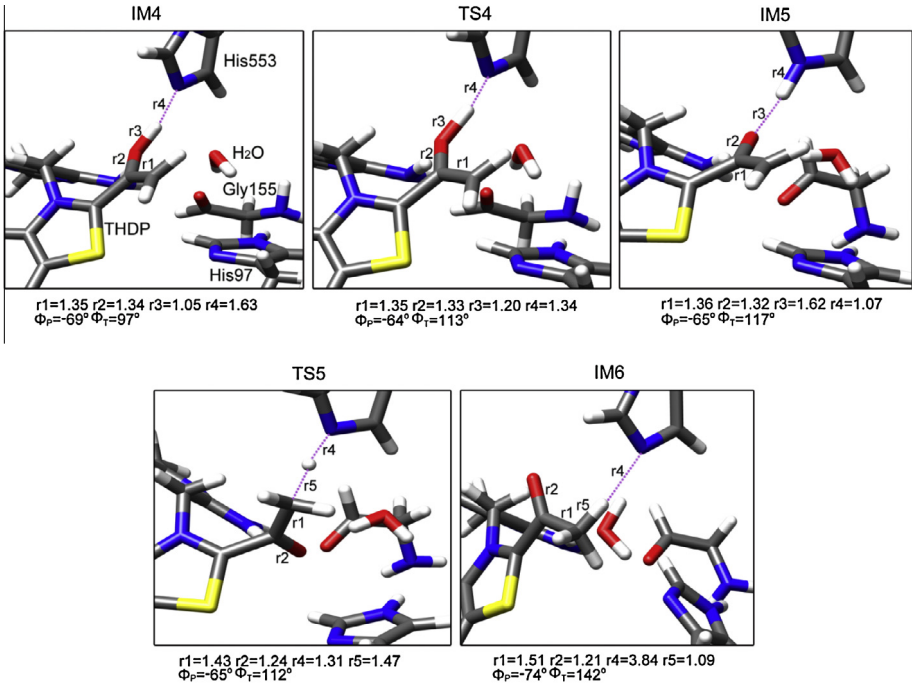

Fig. 6. The truncated active center of the optimized geometries for various species in the Keto–Enol tautomerism obtained at the B3LYP/6-31G(d,p) level. The key bond distances are shown in angstrom and characteristic torsion angles Φ_T and Φ_P for the orientation of the THDP rings are shown in degree.

3.3. Keto–Enol tautomerism

According to experimental studies, the nucleophilic attack by the acceptor substrate (Pi) occurs on the keto form and not on the enol form. Therefore, enolacetyl-THDP (IM4) must firstly undergo the Keto–Enol isomerization (step4 in Scheme 1) to generate AcTHDP, which then participates in the next nucleophilic attack (step5 in Scheme 1). Our calculation results indicate that His553 is probable to play a mediate role in the Keto–Enol tautomerism.

From IM4 in Fig. 6, one can see the hydroxyl group of enolacetyl-THDP forms a hydrogen bond (r4) with His553 with bond length of 1.63 Å, facilitating the proton transfer. In IM5, the hydrogen has completely transferred to His553. The next step is the proton transfer from His553 to the C1″ of enolacetyl-THDP, leading to the formation of AcTHDP (IM6). By comparing the structures of IM4 and IM6 we found that the hydrogen has transferred from the hydroxyl group of enolacetyl-THDP to the C1″ atom via the mediator His553, the Keto–Enol isomerization has been finished. The energy profile is shown in Fig. 4. The energy barrier for the proton transfer from His553 to the C1″ of enolacetyl-THDP is relatively high (25.89 kcal/mol), which is possibly due to the rotation of His553 leading to the increase of strain energy. According to the activation strain model of chemical reactivity [42], the strain energy was calculated to be 37.41 kcal/mol in enzymatic environment, supporting our statement. The computational details of the strain energy are shown in Supporting Information. In addition, the relative energy of AcTHDP (IM6) is 6.53 kcal/mol lower than that of enolacetyl-THDP (IM5), meaning the intermediate AcTHDP (IM6) is more stable. This calculation result is consistent with the experimental proposal that AcThDP is a stable intermediate of PK in the absence of the acceptor (Pi) [7].

4. Conclusions

The main mechanism of PK (steps1–4 in Scheme 1) has been studied by using density functional theory (DFT) method on simplified models. The calculations indicate that the formation of DHETHDP and E4P (step1 and step2) involves one C–C bond formation and one C–C bond cleavage. Each C–C bond formation or cleavage process is always accompanied by a proton transfer between the substrate and histidine residue, but the C–C bond formation or cleavage and the proton transfer is a concerted process but not precisely synchronous. The dehydration process (step3) occurring in the reaction of PK is distinct from that of other THDP-dependent enzymes. The Keto–Enol tautomerism process (step4) is assisted with a mediator His553. His 64, His 553 and His 97 are found to have the function to stabilize the transition states and intermediates. His64 is a better candidate of B1 catalyst. His553 acts as a proton donor to protonate the carbonyl oxygen in step1 and plays intermediary role in the Keto–Enol tautomerism (step4). His97 is the probable B2 catalyst in the dehydration process (step3). By comparing the energy barriers in gas phase and in enzymatic environment by using polarizable-continuum model (PCM), we found that the surrounding environment is crucial for this enzymatic reaction. These results may provide useful information for understanding the reaction mechanism of PK and span the gaps in experiment.

Acknowledgement

This work was supported by the Natural Science Foundation of China (21173129 and 21373125).

Appendix A. Supplementary material

Supplementary data associated with this article can be found, in the online version, at http://dx.doi.org/10.1016/j.comptc.2013.09.026.

References

[1] R.A.W. Frank, F.J. Leeper, B.F. Luisi, Structure, mechanism and catalytic duality of thiamine dependent enzymes, Cell. Mol. Life Sci. 64 (2007) 892–905.
[2] M. Müller, D. Gocke, M. Pohl, Thiamin diphosphate in biological chemistry: exploitation of diverse thiamin diphosphate-dependent enzymes for asymmetric chemoenzymatic synthesis, FEBS J. 276 (2009) 2894–2904.
[3] K. Takahashi, U. Tagami, N. Shimba, T. Kashiwagi, K. Ishikawa, E. Suzuki, Crystal structure of *Bifidobacterium longum* phosphoketolase; key enzyme for glucose metabolism in *Bifidobacterium*, FEBS Lett. 584 (2010) 3855–3861.
[4] R. Suzuki, T. Katayama, B.J. Kim, T. Wakagi, H. Shoun, H. Ashida, K. Yamamoto, S. Fushinobu, Crystal structures of phosphoketolase: thiamine diphosphate-dependent dehydration mechanism, J. Biol. Chem. 285 (2010) 34279–34287.
[5] G. Panagiotou, M.R. Andersen, T. Grotkjaer, T.B. Regueira, G. Hofmann, J. Nielsen, L. Olsson, Systems analysis unfolds the relationship between the phosphoketolase pathway and growth in *Aspergillus nidulans*, PloS One 3 (2008) e3847.
[6] B. Pieterse, R.J. Leer, F.H. Schuren, M.J. van der Werf, Unravelling the multiple effects of lactic acid stress on Lactobacillus plantarum by transcription profiling, Microbiology 151 (2005) 3881–3894.
[7] A. Yevenes, P.A. Frey, Cloning, expression, purification, cofactor requirements, and steady state kinetics of phosphoketolase-2 from Lactobacillus plantarum, Bioorg. Chem. 36 (2008) 121–127.
[8] A. Bairoch, The ENZYME database in, Nucl. Acids Res. 28 (2000) (2000) 304–305.
[9] R.G. Duggleby, Domain relationships in thiamine diphosphate-dependent enzymes, Acc. Chem. Res. 39 (2006) 550–557.
[10] F. Jordan, Current mechanistic understanding of thiamin diphosphate-dependent enzymatic reactions, Nat. Prod. Rep. 20 (2003) 184–201.
[11] N.J. Veitch, D.A. Maugeri, J.J. Cazzulo, Y. Lindqvist, M.P. Barrett, Transketolase from *Leishmania mexicana* has a dual subcellular localization, Biochem. J. 382 (2004) 759–767.
[12] M. Sundström, Y. Lindqvist, G. Schneider, U. Hellman, H. Ronne, Yeast *TKL1* gene encodes a transketolase that is required for efficient glycolysis and biosynthesis of aromatic amino acids, J. Biol. Chem. 268 (1993) 24346–24352.
[13] C. Wikner, U. Nilsson, L. Meshalkina, C. Udekwu, Y. Lindqvist, G. Schneider, Identification of catalytically important residues in yeast transketolase, Biochemistry 36 (1997) 15643–15649.
[14] K.G. Fandi, H.M. Ghazali, A.M. Yazid, A.R. Raha, Purification and N-terminal amino acid sequence of fructose-6-phosphate phosphoketolase from Bifidobacterium longum BB536, Lett. Appl. Microbiol. 32 (2001) 235–239.
[15] J.P. Grill, J. Crociani, J. Ballongue, Characterization of fructose 6 phosphate phosphoketolases purified from Bifidobacterium species, Curr. Microbiol. 31 (1995) 49–54.
[16] R.A.W. Frank, A.J. Price, F.D. Northrop, Crystal structure of the E1 component of the *Escherichia coli* 2-oxoglutarate dehydrogenase multienzyme complex, J. Mol. Biol. 368 (2007) 639–651.
[17] A.K. Steinbach, S. Fraas, J. Harder, A. Tabbert, H. Brinkmann, A. Meyer, U. Ermler, P.M. Kroneck, Cyclohexane-1,2-dione hydrolase from denitrifying Azoarcus sp. strain 22Lin, a novel member of the thiamine diphosphate enzyme family, J. Bacteriol. 193 (2011) 6760–6769.
[18] D. Dobritzsch, S. Konig, G. Schneider, G. Lu, High resolution crystal structure of pyruvate decarboxylase from *Zymomonas mobilis*. Implications for substrate activation in pyruvate decarboxylases, J. Biol. Chem. 273 (1998) 20196–20204.
[19] A. Dawson, M.J. Chen, P.K. Fyfe, Z. Guo, W.N. Hunter, Structure and reactivity of *Bacillus subtilis* MenD catalyzing the first committed step in menaquinone biosynthesis, J. Mol. Biol. 401 (2010) 253–264.
[20] A.K. Bera, L.S. Polovnikova, J. Roestamadji, T.S. Widlanski, G.L. Kenyon, M.J. McLeish, M.S. Hasson, Mechanism-based inactivation of benzoylformate decarboxylase, a thiamin diphosphate-dependent enzyme, J. Am. Chem. Soc. 129 (2007) 4120–4121.
[21] E. Fullam, F. Pojer, T. Bergfors, T.A. Jones, S.T. Cole, Structure and function of the transketolase from Mycobacterium tuberculosis and comparison with the human enzyme, Open Biol. 2 (2012) 110026.
[22] P. Asztalos, C. Parthier, R. Golbik, M. Kleinschmidt, G. Hubner, M.S. Weiss, R. Friedemann, G. Wille, K. Tittmann, Strain and near attack conformers in enzymic thiamin catalysis: X-ray crystallographic snapshots of bacterial transketolase in covalent complex with donor ketoses xylulose 5-phosphate and fructose 6-phosphate, and in noncovalent complex with acceptor aldose ribose 5-phosphate, Biochemistry 46 (2007) 12037–12052.
[23] Q. Pan, Y. Yao, Z.S. Li, Theoretical study of the reaction mechanism of Mycobacterium tuberculosis type II dehydroquinate dehydratase, Comput. Theor. Chem. 1001 (2012) 60–66.
[24] K.M. DiGiovanni, A.K. Hatstat, J. Rote, M. Cafiero, MP2//DFT calculations of interaction energies between acetaminophen and acetaminophen analogues and the aryl sulfotransferase active site, Comput. Theor. Chem. 1007 (2013) 41–47.

[25] M.J. Frisch, G.W. Trucks, H.B. Schlegel, G.E. Scuseria, M.A. Robb, J.R. Cheeseman, J.A. Montgomery, T. Vreven, K.N. Kudin, J.C. Burant, J.M. Millam, S.S. Iyengar, J. Tomasi, V. Barone, B. Mennucci, M. Cossi, G. Scalmani, N. Rega, G.A. Petersson, H. Nakatsuji, M. Hada, M. Ehara, K. Toyota, R. Fukuda, J. Hasegawa, M. Ishida, T. Nakajima, Y. Honda, O. Kitao, H. Nakai, M. Klene, X. Li, J.E. Knox, H.P. Hratchian, J.B. Cross, V. Bakken, C. Adamo, J. Jaramillo, R. Gomperts, R.E. Stratmann, O. Yazyev, A.J. Austin, R. Cammi, C. Pomelli, J.W. Ochterski, P.Y. Ayala, K. Morokuma, G.A. Voth, P. Salvador, J.J. Dannenberg, V.G. Zakrzewski, S. Dapprich, A.D. Daniels, M.C. Strain, O. Farkas, D.K. Malick, A.D. Rabuck, K. Raghavachari, J.B. Foresman, J.V. Ortiz, Q. Cui, A.G. Baboul, S. Clifford, J. Cioslowski, B.B. Stefanov, G. Liu, A. Liashenko, P. Piskorz, I. Komaromi, R.L. Martin, D.J. Fox, T. Keith, M.A. Al-Laham, C.Y. Peng, A. Nanayakkara, M. Challacombe, P.M.W. Gill, B. Johnson, W. Chen, M.W. Wong, C. Gonzalez, J.A. Pople, Gaussian 03, 2004.
[26] G.M. Morris, D.S. Goodsell, R.S. Halliday, Automated docking using a Lamarckian genetic algorithm and an empirical binding free energy function, J. Comput. Chem. 9 (1998) 1639–1662.
[27] V. Barone, M. Cossi, J. Tomasi, Geometry optimization of molecular structures in solution by the polarizable continuum model, J. Comput. Chem. 19 (1998) 404–417.
[28] J. Tomasi, M. Persico, Molecular interactions in solut ion: an overview of methods based on continuous distributions of the solvent, Chem. Rev. 94 (1994) 2027–2094.
[29] L. Noodleman, T. Lovell, W.G. Han, J. Li, F. Himo, Quantum chemical studies of intermediates and reaction pathways in selected enzymes and catalytic synthetic systems, Chem. Rev. 104 (2004) 459–508.
[30] F. Himo, Quantum chemical modeling of enzyme active sites and reaction mechanisms, Theor. Chem. Acc. 116 (2006) 232–240.
[31] J.J. Robinet, K.B. Cho, J.W. Gauld, A density functional theory investigation on the mechanism of the second half-reaction of nitric oxide synthase, J. Am. Chem. Soc. 130 (2008) 3328–3334.
[32] P.E.M. Siegbahn, F. Himo, Recent developments of the quantum chemical cluster approach for modeling enzyme reactions, J. Biol. Inorg. Chem. 14 (2009) 643–651.
[33] O. Amata, T. Marino, N. Russo, M. Toscano, A proposal for mitochondrial processing peptidase catalytic mechanism, J. Am. Chem. Soc. 133 (2011) 17824–17831.
[34] D. Kern, G. Kern, H. Neef, K. Tittmann, M. Killenberg-Jabs, C. Wikner, G. Schneider, G. Hübner, How thiamine diphosphate is activated in enzymes, Science 275 (1997) 67–70.
[35] G. Hübner, K. Tittmann, M. Killenberg-Jabs, J. Schäffner, M. Spinka, H. Neef, D. Kern, G. Kern, G. Schneider, C. Wikner, S. Ghisla, Activation of thiamin diphosphate in enzymes, Biochim. Biophys. Acta 1385 (1998) 221–228.
[36] K. Tittmann, K. Mesch, M. Pohl, G. Hübner, K. Tittmann, K. Mesch, M. Pohl, G. Hübner, Activation of thiamine diphosphate in pyruvate decarboxylase from *Zymomonas mobilis*, FEBS Lett. 441 (1998) 404–406.
[37] A. Bar-Ilan, V. Balan, K. Tittmann, R. Golbik, M. Vyazmensky, G. Hübner, Z. Barak, D.M. Chipman, Binding and activation of thiamin diphosphate in acetohydroxyacid synthase, Biochemistry 40 (2001) 11946–11954.
[38] B. Shaanan, D.M. Chipman, Reaction mechanisms of thiamin diphosphate enzymes: new insights into the role of a conserved glutamate residue, FEBS J. 276 (2009) 2447–2453.
[39] R. Friedemann, K. Tittmann, R. Golbik, G. Hübner, DFT and MP2 studies on the C2–C2α bond cleavage in thiamin catalysis, J. Mol. Catal. B 61 (2009) 36–38.
[40] J.Y. Wang, H. Dong, S.H. Li, H.W. He, Theoretical study toward understanding the catalytic mechanism of pyruvate decarboxylase, J. Phys. Chem. B 109 (2005) 18664–18672.
[41] S. Chakraborty, N. Nemeria, A. Yep, M.J. McLeish, G.L. Kenyon, F. Jordan, Mechanism of benzaldehyde lyase studied via thiamin diphosphate-bound intermediates and kinetic isotope effects, Biochemistry 47 (2008) 3800–3809.
[42] W.J. van Zeist, F.M. Bickelhaupt, The activation strain model of chemical reactivity, Org. Biomol. Chem. 8 (2010) 3118–3127.